Title
Survival and Functional Integration of Human Embryonic Stem Cell—Derived Retinal Organoids After Shipping and Transplantation into Retinal Degeneration Rats

Journal
Stem Cells and Development, 33(9-10)

ISSN
1547-3287

Authors
Lin, Bin
Singh, Ratnesh K
Seiler, Magdalene J
et al.

Publication Date
2024-05-01

DOI
10.1089/scd.2023.0257

Stem Cells and Development

DOI: 10.1089/scd.2023.0257

Survival and functional integration of human embryonic stem cell-derived retinal organoids after shipping and transplantation into retinal degeneration rats

Bin Lin[1], Ratnesh K. Singh[2], Magdalene J. Seiler[1]✶, Igor O. Nasonkin[2#]✶

[1]University of California, Irvine; School of Medicine, Physical Medicine & Rehabilitation; Ophthalmology; Sue & Bill Stem Cell Research Center, 845 Health Sciences Rd.; 2035 Gross Hall, Irvine, CA 92697-1705; [2]Lineage Cell Therapeutics, Inc., :2173 Salk Avenue, Suite 200, Carlsbad CA 92008; [#] current affiliation: Phythera Therapeutics, LLC, San Leandro, CA 94577

✶ Co-corresponding authors

Word count: Abstract: 250 words; Text without references and Acknowledgments: 3744 words; 8 Figures, 2 Supplemental tables; 2 Supplemental figures

Running title:

hESC-retinal grafts to immunodeficient blind rats

Corresponding author:
Magdalene Seiler

University of California, Irvine

845 Health Sciences Rd.; Irvine CA 92697

e-mail: mseiler@uci.edu; Tel. 949-824-2037

ORCID IDs:
BL: 0000-0001-7043-5788

RKS: 0000-0002-7085-447X

MJS: 0000-0002-0869-9923

ION: 0000-0002-9286-2219

Stem Cells and Development

Survival and functional integration of human embryonic stem cell-derived retinal organoids after shipping and transplantation into retinal degeneration rats (DOI: 10.1089/scd.2023.0257)

This paper has been peer-reviewed and accepted for publication, but has yet to undergo copyediting and proof correction. The final published version may differ from this proof.

Abstract

Because derivation of retinal organoids (ROs) and transplantation are frequently split between geographically distant locations, we have developed a special shipping device and protocol capable of the organoids' delivery to any location. Human embryonic stem cell (hESC) derived ROs were differentiated from the hESC line H1 (WA01), shipped overnight to another location, and then transplanted into the subretinal space of blind immunodeficient retinal degenerate (RD) rats. Development of transplants was monitored by spectral-domain optical coherence tomography. Visual function was accessed by optokinetic tests and superior colliculus (SC) electrophysiology. Cryostat sections through transplants were stained with hematoxylin & eosin; or processed for immunohistochemistry to label human donor cells, retinal cell types and synaptic markers. After transplantation, ROs integrated into the host RD retina, formed functional photoreceptors, and improved vision in the rats with advanced RD. The survival and vision improvement are comparable with our previous results of hESC-ROs without a long-distance delivery. Furthermore, for the first time in the stem cell transplantation field, we demonstrated that the response heatmap on the SC showed a similar shape to the location of the transplant in the host retina, which suggested the point-to-point projection of the transplant from the retina to SC. In conclusion, our results showed that using our special device and protocol, the hESC derived ROs can be shipped over long distance and are capable of survival and visual improvement after transplantation into the RD rats. Our data provide a proof-of concept for stem cell replacement as a therapy for RD patients.

Keywords: retinal degeneration, cell therapy, retinal organoids, tissue replacement, subretinal transplantation, synaptic integration

Introduction

Blindness causes major emotional burden to patients and economic burden to society [1,2]. Blindness resulting from photoreceptor (PR) cell death is currently incurable, an urgent unmet medical need [2-10]. Retinal degenerative (RD) diseases which lead to PR degeneration are the third leading cause of worldwide blindness. Age-related Macular Degeneration (AMD), a leading cause of RD in people over 60 years in developed countries, affects about 15 million people in the US, with the number projected to double by 2030 [5,6,10]. Retinitis pigmentosa (RP) is the most frequent cause of inherited visual impairment, affecting about 100,000 people in the US and 1.5 million people worldwide [9,11-14].

Retinal repair is a major challenge with no currently available solutions, especially in the cases of advanced RD. Aside from anti-VEGF antibody treatment, there are no drugs that can substantially repair retinal damage. Preservation of retinal layered neuroanatomical structure and synaptic networks are needed to maintain visual function.

Restoring photoreceptors is a major therapeutic goal to alleviate blindness. Among all cell replacement therapies, retinal stem cell therapy stands out because it is one of the most technically feasible cell therapies. The ocular space is accessible through trans-vitreal [4,15] or trans-scleral [16] injection. Furthermore, subretinal grafts can be easily visualized using noninvasive methods [17-19]. Vitreoretinal surgery in large-eye animal models, though technically demanding, is a routine and established procedure, with many ongoing innovations and new tools and equipment described each year [17,18,20-22].

The relative retinal immune privilege enables long-term maintenance of allogeneic (non-autologous) cells and tissues (e.g., PRs [4,23,24] and retinal tissue grafts [25,26]). Advances in regenerative medicine enabled generation of 3-dimensional retinal organoids (ROs) from pluripotent stem cells, closely recapitulating the biological complexity and physiology of human retina [27-33]. This created new opportunities for cell replacement therapies and provides us with unlimited supply of clinical-grade retinal cells and tissue for 3D subretinal implants.

Research in the past 20 years indicates that retina can be replaced by fetal tissue (8-17 weeks of human gestation) [25,34]. We have demonstrated that human fetal tissue at this

age is almost identical to hESC-retinal tissue based on cellular composition and lamination (critical for biological function) [31,35]. A major advantage of retinal replacement technology is that semi-differentiated retinal tissue maintains the original lamination and cell fate commitment when transplanted as a 3D sheet. This happens even in cases when retinal tissues are grafted in the eye with advanced RD [34,36,37] and allows preservation of the developing neuroanatomical circuitry of hESC-retina, which is not the case with PR cells delivered as a suspension of cells into the subretinal space [4,38]. The immature retinal tissue continues differentiation and establishes functional connectivity with the recipient's retinal circuitry and the visual cortex after grafting [39-42].

In vivo validation and refinement of any vision restoration technique in RD animal models is mandatory before clinical trials. We earlier reported vision improvements in two established RD rat models with retinal tissue implants from hESC line CSC-14 [19,43]. Here we expand our work by testing hESC-retina derived from the commonly used hESC line H1 (WA01) [33] and also report the improvement of vision in rats with advanced RD, immunodeficient *RhoS334ter-3* rats [44] that have lost most rod photoreceptors at the age of 4 weeks and never develop outer segments [45,46]. Our results validate the safe use of hESC-derived retinal tissue as alternative to human fetal retina to restore vision in eyes with complete photoreceptor loss, irrespective of the stem cell source. This work brings us closer to initiating testing of this promising technology in patients with advanced RD.

Methods:

Cell Culture

Retinal organoids (ROs) were generated from hESC line H1 (WA01) [31] as we earlier reported [33] and closely resembled ROs previously used for transplantation [18]. hESC colonies were allowed to grow for 6-8 days in mTeSR1, then (when they reached ~40-50% density) neuralized using human noggin (100 ng/ml) and Neurobasal complete medium (with N2 and B27, as we described). Well-defined retinal structures were dissected out from the differentiating monolayer (at ~week 7-8) using a sharp sterile glass rod pulled from a Pasteur pipette, and further maintained in suspension in 6-well plates in an incubator with slow agitation (linear shaker) until reaching the age of 70 days.

Shipping Retinal Organoids with portable device

Organoids were collected from suspension cultures and placed into a 15-ml culture tube with media which was placed and secured horizontally into the shipping device. We used a battery-driven portable shipper with 0.028-m^3 capacity (manufacturer: Uline, Part Number S-20589, Model Number 20589) [47]. Two types of tracking devices were used to track the temperature, G-forces and the GPS location [47]. The device was placed into a FEDEX-approved shipping crate labelled with "UN3373" (Category B biological substance), "do not X-ray" stickers and "up" arrows.

The ROs were shipped at 37°C by Fedex overnight to arrive the next morning (FEDEX Priority overnight) from a stem cell facility in Alameda, CA to UC Irvine without loss of viability (as we previously reported [47]) and prepared for transplantation. The organoids were immediately placed into an incubator upon arrival, followed by examination under a cell culture microscope. Surgery was usually 1-2 days later. Organoids not used for transplantation were fixed and analyzed later. As a batch control for each RO lot used for retinal surgeries, we differentiated a few randomly selected ROs for further characterization at 3-4 months. Immunohistochemistry delineated the distribution of early retinal markers in retinal organoids [33].

Experimental Animals

Animals were treated in accordance with NIH guidelines for the care and use of laboratory animals, the ARVO Statement for the Use of Animals in Ophthalmic and Vision Research, and under a protocol approved by the Institutional Animal Care and Use Committee of UC Irvine. *SD-Foxn1 Tg(S334ter)3Lav* (RD nude rat) transplant recipients were generated by crossing *SD-Tg(S334ter)3Lav* rats and *NTac:NIH-Whn* rats [44].

Retina Sheet Preparation

ROs (day 70 of differentiation) were selected based on transparency, and morphology of a hollow spherical shape with a laminated structure seen under phase contrast and stereoscope. Structures often contained adherent RPE aggregates that were removed during the preparation of retinal rectangular sheets (1.0-1.7x 0.6 mm) for transplantation.

The rims of ROs (carrying a layer of human developing PRs) were then dissected for transplantation (**Supplemental Fig.1**).

Transplantation

Recipient rats (P27-45, either sex) were randomized into age-matched non-surgery (AMC) (n=11), sham (n=7), and transplant (n=56) experimental groups.

Rats received a subcutaneous injection of Ketoprofen (4mg/kg) (Parsippany-Troy Hills, NJ) and dexamethasone eye drops (Bausch & Lomb Inc., Rancho Cucamonga, CA) prior to anesthesia to prevent eyelid swelling. After ketamine/xylazine anesthesia (40-55 mg/kg Ket, 6.0 – 7.5 mg/kg Xyl), pupils were dilated by 1% atropine eye drops (Akorn, Lake Forest IL). Eyes were disinfected with ophthalmic betadine (Alcon, Fort Worth, TX). Nonsurgical eyes were kept moist by artificial tears (Akorn). During surgery, the eye was frequently treated with 0.5% tetracaine (Bausch & Lomb) and 0.1% dexamethasone eye drops (Bausch & Lomb).

Transplantation of retinal sheets has been previously described [39,43]. Briefly, a small incision (~1 mm) was made posterior to pars plana, parallel to the limbus, followed by local retinal detachment. Using a custom implantation instrument, donor tissue was gently placed into the subretinal space of the left eye. Media alone was injected into the eyes of sham surgery rats. The incision was closed with 10-0 sutures. Eyes were examined by fundoscopy immediately after surgery. For recovery, gentamycin/polymycin/bacitracin ointment (Bausch & Lomb) was applied to the surgical eyes.

Spectral Domain Optical Coherence Tomography (SD-OCT) Imaging

SD-OCT imaging (Bioptigen Envisu R2200; Bioptigen, Research Triangle Park, NC) was used to document and monitor transplant development, as described previously [34,39]. Transplanted rats (n=56) were imaged every 1-2 months, starting 2 weeks after surgery, up to 8.9 months of age (7.5 months post-surgery). Rats with transplant misplacement into the vitreous, or excessive surgical trauma were excluded from further analysis. The last scan was scheduled as close as possible to the terminal SC recording.

Stem Cells and Development
Survival and functional integration of human embryonic stem cell-derived retinal organoids after shipping and transplantation into retinal degeneration rats (DOI: 10.1089/scd.2023.0257)
This paper has been peer-reviewed and accepted for publication, but has yet to undergo copyediting and proof correction. The final published version may differ from this proof.

Stem Cells and Development
Survival and functional integration of human embryonic stem cell-derived retinal organoids after shipping and transplantation into retinal degeneration rats (DOI: 10.1089/scd.2023.0257)
This paper has been peer-reviewed and accepted for publication, but has yet to undergo copyediting and proof correction. The final published version may differ from this proof.

The transplant area was determined by using sequential cross-sectional B-scans to define the host/donor boundary. These positions were then compared to the corresponding locations in the fundus image to outline the transplant (**Figure 2 c,f,i**). The InVivoVue program (Bioptigen) contains calipers that were used to create several geometric figures to overlay the transplant border.

Optokinetic Response Testing (OKT)

After at least 1 hour dark-adaption, the visual acuity of transplanted, sham surgery, and non-surgery AMC control rats was measured by recording optomotor responses to a virtual cylinder with alternating black and white vertical stripes at 6 different spatial frequencies (Optomotry, Cerebral Mechanics, Alberta, Canada) at 1, 2 and 4 months post-surgery (MPS), as previously described [39,43]. Tests were videotaped and evaluated off-line by two independent observers blinded to the experimental condition. The best visual acuity of the two same-day tests was used for analysis. If there was a discrepancy between the two observers, videos were re-analyzed by a third observer. All testers and video-watchers were blinded to the experimental group assignment of rats.

Superior Colliculus (SC) Electrophysiological recording

Visual responses from the SC were recorded as previously described [34,39] after overnight dark-adaption, at the age of 6.4-8.9 months (5.1-7.4 months after surgery). Multi-unit electrical responses from approximately 50 locations on the SC surface, 200-400 µm apart, using a tungsten microelectrode (0.5 MΩ impedance; MicroProbe, Inc., Carlsbad, CA). At each location, light stimuli (20 ms, + 0.58 to – 6.13 log cd/m^2) were delivered 10-times at 10-second-intervals. When responses were found, intensity of light stimuli was reduced to determine the response threshold. Responses to the strongest light stimuli (stimulus level 0.58 log cd/m^2) were quantified into a map over the area of the SC. All spikes occurring 30 ms to 210 ms after the onset of the photic stimulus were counted. Spike counts and locations of responses were analyzed using a custom MATLAB program (Mathworks, Natick, MA).

Histology and Immunofluorescence

After euthanasia with injection of anesthetic overdose, rats were perfusion-fixed with cold 4% paraformaldehyde in 0.1 M Na-phosphate buffer. After opening the cornea, eyes were post-fixed overnight at 4°C, then washed. Eye cups were dissected along the dorso-ventral axis, cryoprotected (30% sucrose) and frozen in O.C.T. compound. ROs were frozen using a similar procedure. Serial 10µm cryostat sections were stored at -20°C. Every fifth slide was stained using hematoxylin and eosin (H&E) and imaged on an Olympus BXH10 using an Infinity 3-1U camera. For immunofluorescence and diaminobenzidine (DAB) analysis, cryostat sections underwent antigen retrieval at 70 °C with Histo-VT One (Nacalai USA Inc., San Diego, CA), followed by PBS washing, blocking with 20% goat serum, and primary antibodies overnight at 4°C. Slides were incubated for 30-60 min at room temperature in fluorescent or biotinylated secondary antibodies. Primary and secondary antibodies are listed in **Supplemental Table 1**. Fluorescent sections were coverslipped using Vectashield mounting media (Vector Labs, Burlingame, CA) with 5 µg/mL DAPI (4,6-Diamidino-2-phenylindole).

For DAB (3',3'-diaminobenzidine) staining, sections were incubated with ABC kit (Vector Labs, Burlingame, CA) after the biotinylated secondary antibody and developed with DAB for up to 4 minutes.

A Zeiss LSM700 or LSM900 confocal microscope (Zeiss, Oberkochen, Germany) was used for imaging fluorescent images (tiled stacks of 5-8 micron thickness at 20x and 40x). Confocal images were extracted in Zen 2012 and 2.3 software (Zeiss, Oberkochen, Germany). 3D images were extracted separately for each channel and combined in Adobe Photoshop CS6 to Photoshop 2023/2024 software (San Jose, CA). Imaris software (Oxford instruments) was also used for 3D rendering and to analyze colocalization (closeness defined as a distance of 1µm or less) (see **Fig. 7**).

Statistical Analysis

For all statistical analyses, the significance level was calculated in GraphPad Prism software (Graphpad Software LLC, La Jolla, CA) with paired and unpaired two-tailed t-tests using mean ± SEM. Level of significance was set at 0.05.

Stem Cells and Development
Survival and functional integration of human embryonic stem cell-derived retinal organoids after shipping and transplantation into retinal degeneration rats (DOI: 10.1089/scd.2023.0257)
This paper has been peer-reviewed and accepted for publication, but has yet to undergo copyediting and proof correction. The final published version may differ from this proof.

RESULTS

Some transplanted animals were used only for histology and not for functional tests to investigate transplant development. Some rats were eliminated from analysis after the first or second OCT exam because of faulty surgeries (e.g., optic nerve damage, choroid damage, or epiretinal placement of the transplant) or corneal ulcers. Four transplant rats could not be used for the final analysis because they died before recording.

Development and characterization of ROs

An example of organoid development at the time of transplantation is shown in **Figure 1**. Organoids developed some level of laminated structure. As previously reported, at the time of transplantation, the donor tissue had no mature photoreceptors, as determined by qPCR and histology (data not shown and **Figure 1**). The retinal organoids also had no mature cones (Opsin+) or rods (Rhodopsin+) at this stage but contained photoreceptor precursors (Crx+) (**Figure 1d**).

In vivo development of retinal organoid transplants monitored by OCT

Rat eyes were imaged by optical coherence tomography imaging (OCT) to check initially for the presence of the graft at 2 and 4 weeks post-transplantation, and then for graft expansion and lamination every 2 months up to 6 MPS. Initial transplant size was 0.6 to 0.84 mm^2. Transplants matured and developed into rosettes several months post transplantation (**Figure 2 g,h**). Examples of OCT images are shown in Figure 2 with arrows pointing out the hyper-reflective photoreceptor rosettes within transplants (**Figure 2 g,h**). Transplant morphology in OCT scans corresponded to that seen in H-E stained sections (**Supplemental Figure 2**).

Visual function improvement evaluated by optokinetic testing (OKT)

Visual acuity significantly decreased with age in non-surgery AMC RD rats (n=11) and sham surgery RD rats (n=6) (**Figure 3**). There was no significant difference between left eye (LE) and right eye (RE) in sham surgery and AMC groups, and no difference between AMC and sham control rats. In addition, the right non-surgery eyes of the transplanted rats (n=14) showed the same degree of visual acuity loss as non-surgery AMC and sham surgery rats.

At 1 month post-surgery (MPS), the transplanted eyes showed improvement compared to the non-surgery right eyes of the same rats but not significant because of low N, while the transplanted eyes showed significant improvement compared to non-surgery AMC and sham surgery rats. This difference became larger at later time points (**Figure 3**). The improvement was also significant compared to non-surgery AMC ($P<0.05$; **Figure 3**).

Visual function improvement evaluated by SC electrophysiological recording

After transplantation, at the age of 6.4 – 8.9 months, 4 of 5 rats showed responses to flashes of light in the SC (**Figure 4; Supplemental Table 2**). Four transplanted rats showed responses to dimmer light (the best light threshold was -0.16 log cd/m^2 (**Supplemental Table 2; Figure 4c-f**). No responses could be evoked in any SC area of control non-surgery AMC rats (n=9) (**Figure 4a**) and sham surgery rats (n=7) (**Figure 4b**) at the maximum light level (+ 0.58 log cd/m^2). The vision improvement demonstrated in the transplanted group was significant compared to AMC and sham surgery groups ($P<0.05$). Interestingly, in one of the transplants, the SC response heatmap showed the similar shape as the transplant location in the eye, which suggested that the transplant restore the basic point to point projection function from eye to the SC (**Figure 4c**).

Immunohistochemical analysis of transplant cell type development

After transplantation, the human nuclear marker Ku80 (**Figure 5 a-d**) and human-specific synaptophysin (**Figure 6**) confirmed the distribution of transplanted tissue within the host subretinal space. Some donor cells migrated into the host retina (**Figure 5 a-d**). We further characterized the 5.1-7.4-month hESC-RO grafts in rats with SC responses by an array of immunohistochemical markers to developing and mature PRs (**Figure 5, 6**): Retinal organoids produced photoreceptors immunoreactive for recoverin (**Figure 5 g,j,k, Figure 6a**), Red-Green Opsin+ cones (**Figure 5b,c**) , Rhodopsin+ rods (**Figure 5d-f, h, i**), and organized into rosettes with putative outer segments elongating and maturing over time.

Synaptic connectivity

Transplant and host cells formed synaptic connections as shown by antibodies specific for calretinin, human synaptophysin (synaptic vesicles), in combination with rodent-specific α-synuclein (rodent IPL **Figure 6a,b; Figure 7**). A rodent-specific α-synuclein antibody (**Figure**

Stem Cells and Development
Survival and functional integration of human embryonic stem cell-derived retinal organoids after shipping and transplantation into retinal degeneration rats (DOI: 10.1089/scd.2023.0257)
This paper has been peer-reviewed and accepted for publication, but has yet to undergo copyediting and proof correction. The final published version may differ from this proof.

6) demonstrated intermingling of transplant (human synaptophysin) and host (α-synuclein) processes in the host inner plexiform layer (IPL), (**Figure 7**). Imaris image analysis of the host IPL with triple staining for calretinin, human-specific synaptophysin and rodent α-synuclein (**Figure 7**) demonstrated co-localization ("closeness") of all 3 markers in the host IPL. Overall, in transplants #1-#4, about 2.11±0.34% of rodent α-synuclein dots were colocalized with human synaptophysin immunoreactive spots, and 3.87±0.59% of synaptophysin immunoreactive spots in the host IPL were colocalized with rodent α-synuclein.

Discussion

We have developed a successful overnight retinal organoid shipping protocol, which provided reliable temperature control and live monitoring of the shipment conditions. This allows for differentiating the best (transplantation-competent) hPSC-derived ROs in a special facility, and then shipping them over large distances to any hospital over the world for transplantation on the patients there. Our data showed the efficient and tumor-free engraftment of hESC-derived human retinal tissue (from ROs) after long distance shipping, which is a good starting point for developing clinical-grade retinal tissue implants for restoring vision in profoundly blind patients with significant loss of photoreceptors. Our grafts survived in subretinal space for more than 6 months, developed mature PRs with inner and outer segments, established dense array of graft-with-host synapses in the host INL and RGC layers, and critically, reproducibly improved vision in the blind recipient animals with completely degenerated PRs. These results corroborated our earlier data in the same rat model with a different hESC line as source of retinal grafts [43].

Correlation of vision improvement with transplant location in the retina

hESC-retinal tissue transplanted to rats with RD induced vision improvement, evident on optokinetic test (OKT; visual acuity test) and activation of contralateral superior colliculus, but not in retina with sham surgery or no surgery. Interestingly, in one of the transplants, the SC response heatmap showed the similar shape as the transplant location in the eye, which suggested that the transplant restored the basic point to point projection function from the eye to the SC (**Fig. 4**).

Importance of rat model

Recipient rats were immunodeficient (RD nude) animals without T cells (not capable of rejecting xenografts) and the *S334ter* rhodopsin mutation which causes complete PR degeneration by 3-4 months after birth [44]. Therefore, no immunosuppressants were needed to enable graft survival. Immunodeficiency and lack of PRs in the recipient eyes eliminated the always present concerns about the survival of xenogeneic human grafts in animal models and the presence of some functional host PRs. Such concerns could lead to skewing the *in vivo* results and confounding the overall readout of the efficacy. We have previously shown that optokinetic responses in this rat are already severely reduced at the age of 23-27d [43]. The RD nude rat model, therefore, is a superb model for demonstrating the preclinical efficacy of our vision restoration technology.

Challenges of surgery

The small eyes and the large lens of RD nude rats present a challenge for surgical grafting. Due to this, we had a number of unsuccessful surgeries, where the animals had to be terminated due to (mostly) developing cataracts resulting from the surgical instrument inadvertently damaging the lens (most frequent case) or the degenerating retina. The surgery had to be done without the ability to clearly see the intravitreal space and the retina, thus complicating the overall precision and placement of a slice of hESC-retina into a subretinal space. Critically, all the above issues are not applicable in a much larger eye of a human patient where complex vitreoretinal procedures like subretinal surgeries have been worked out [20,48].

Source and maturation of retinal tissue

Here we used H1 (WA-01) hESC line (WiCell) as a source of human retinal tissue for subretinal grafting. We recently reported the derivation of hESC-ROs from hESC line H1 [31,33].

Our approach demonstrates efficient derivation of retinal tissue from hESCs carrying all the essential markers of developing human fetal retina including rod and cone photoreceptors (Figure 5), resembling developing human retina of developmental age 10-13 weeks [33].

Stem Cells and Development

Survival and functional integration of human embryonic stem cell-derived retinal organoids after shipping and transplantation into retinal degeneration rats (DOI: 10.1089/scd.2023.0257)

This paper has been peer-reviewed and accepted for publication, but has yet to undergo copyediting and proof correction. The final published version may differ from this proof.

This is important because human fetal retina of similar age has been used in a successful phase 2 clinical trial of RP and AMD, which reported vision improvements in several patients [25]. Upon maturation, hESC-derived retinal tissue (ROs) revealed the presence of a dense PR layer with mitochondria-rich inner segments, connecting cilia, and developing outer segments [33]. Collectively, this indicates that the grafts placed in the subretinal space of RD nude animals could similarly develop mature PRs, one of the critical mandatory requirements to restore vision.

Immunohistochemical analysis of subretinal grafts in rats with vision improvement (OKT improvement, SC activation) after transplantation reveals presence of RHO [+], RCVRN [+] outer segment-like protrusions from photoreceptors in the graft. Interestingly, in one of the transplants, the SC response heatmap showed a similar shape as the transplant in the eye, which suggested that the transplant restored the basic point to point projection function from eye to the SC (Fig 3).

Synaptic connectivity

Using donor and host-specific markers in combination with synaptic markers also showed that transplants extend neuronal processes into the inner plexiform layer of the host retina. Imaris software analysis showed co-localization of these markers, indicating synaptic connectivity between transplant and host. In addition, some donor cells migrated into the host retina. These results are similar to previous results using retinal organoids from a different cell line [19,43]. However it is still unknown which specific cell types are involved.

Limitations of the study

Our study showed that transplanted retinal organoids can have similar effects on the vision of a retinal degenerate recipient when shipped long-distance as tissue received from a close location. However, it was not possible to have a parallel control group on non-shipped RO transplants as the company producing the organoids has no facilities for rat housing and surgery.

Grafted sheets of photoreceptors from hESC-derived retinal tissue may improve vision. Vision improvements remain so far small, but with additional improvements of grafts, this approach has the potential to restore vision to RD retina with no remaining PRs.

Future work should be focused on generating grafts in large RD models, improving functional integration to achieve better SC responses, studying vision restoration in the translational large eye models with RD and developing additional functional tests, such as cortical recordings, visual evoked potentials (VEP) etc., enabling translation of preclinical efficacy results to clinical trials in patients with profound/total vision loss.

Conclusions

The data show that hESC-derived retinal tissue has a promise in restoring vision in the eyes with total loss of vision and photoreceptors. These results, together with results from other publications [19,43,49-51] support the development of the stem cell replacement therapy in vision restoration and testing this technology in future clinical trials.

Acknowledgments:

Supported by NIH 1R44EY027654, NEI 3 R44EY 027654 - 02S1 (PI IN, MPI MJS); NIH R01 EY031834 (PI MJS); CIRM TR1-10995 (PI MJS). This study was made possible in part through access to the Optical Biology Core Facility of the Developmental Biology Center, a shared resource supported by the Cancer Center Support Grant (CA-62203) and Center for Complex Biological Systems Support Grant (GM-076516) at the University of California, Irvine. The authors acknowledge support to the Gavin Herbert Eye Institute at the University of California, Irvine from an unrestricted grant from Research to Prevent Blindness and from NIH grant P30 EY034070.

The authors wish to thank the late Dr. Robert Aramant for his contributions to the project and Dr. Robert Fariss, National Eye Institute, for technical assistance.

The authors wish to thank staff members Robert Sims, Juri Pauley, Amr Azzam, Tej Kalakuntla, Johanes Santoso; Graduate student Yuntian Xue, and Undergraduate students

Luxi Zhang, Derek C.Y. Lee, Catherine Kloesel, Reeva Reyes, Kevin Ivan Sanchez, Evelyn Dao, Ethan Teng, Lesley Wong, Marisa Kin, William Le, Johnny Garcia, Sarina Vang, Judy Ly, Lindsay Kung, Neelakshi Patne, Angela Davidian, Palak Verma, Disha Patel, Ryan Pavey, Caroline Lee, Angel Blanquel, Kevin Wu, Johnell Amoroso, Mia Isabelle Castro and many other students for technical assistance.

Consent to participate: all authors have consented to participate.

Consent for publication: all authors have approved the publication.

Data availability statement: Additional data available upon request.

Code availability: Matlab code for analysis of superior colliculus responses is available upon request

Conflicts of Interest/Competing Interests:

The authors declare no competing interests.

Funding:

NIH 1R44EY027654 (PI IN, MPI: MJS);

NEI 3 R44EY 027654 - 02S1 (PI IN, MPI: MJS);

NIH R01 EY031834 (PI MJS);

CIRM TR1-10995 (PI MJS)

Ethics approval:

IACUC protocol AUP18-145 (UC Irvine); hSCRO protocol: 2006-5316 UC Irvine; no human subjects involved

References

1. Bastawrous A and AV Suni. (2020). Thirty Year Projected Magnitude (to 2050) of Near and Distance Vision Impairment and the Economic Impact if Existing Solutions are Implemented Globally. Ophthalmic Epidemiol 27:115-120.

2. Pascolini D, SP Mariotti, GP Pokharel, R Pararajasegaram, D Etya'ale, AD Negrel and S Resnikoff. (2004). 2002 global update of available data on visual impairment: a compilation of population-based prevalence studies. Ophthalmic Epidemiol 11:67-115.

3. Veleri S, CH Lazar, B Chang, PA Sieving, E Banin and A Swaroop. (2015). Biology and therapy of inherited retinal degenerative disease: insights from mouse models. Dis Model Mech 8:109-29.

4. Hambright D, KY Park, M Brooks, R McKay, A Swaroop and IO Nasonkin. (2012). Long-term survival and differentiation of retinal neurons derived from human embryonic stem cell lines in un-immunosuppressed mouse retina. Mol Vis 18:920-36.

5. Friedman DS, BJ O'Colmain, B Munoz, SC Tomany, C McCarty, PT de Jong, B Nemesure, P Mitchell, J Kempen and G Eye Diseases Prevalence Research. (2004). Prevalence of age-related macular degeneration in the United States. Arch Ophthalmol 122:564-72.

6. Jager RD, WF Mieler and JW Miller. (2008). Age-related macular degeneration. N Engl J Med 358:2606-17.

7. Hartong DT, EL Berson and TP Dryja. (2006). Retinitis pigmentosa. Lancet 368:1795-809.

8. Christensen R, Z Shao and DA Colon-Ramos. (2013). The cell biology of synaptic specificity during development. Curr Opin Neurobiol 23:1018-26.

9. Duncan JL, EA Pierce, AM Laster, SP Daiger, DG Birch, JD Ash, A Iannaccone, JG Flannery, JA Sahel, DJ Zack, MA Zarbin and B and the Foundation Fighting Blindness Scientific Advisory. (2018). Inherited Retinal Degenerations: Current Landscape and Knowledge Gaps. Transl Vis Sci Technol 7:6.

10. Rein DB, JS Wittenborn, Z Burke-Conte, R Gulia, T Robalik, JR Ehrlich, EA Lundeen and AD Flaxman. (2022). Prevalence of Age-Related Macular Degeneration in the US in 2019. JAMA Ophthalmol 140:1202-1208.

11. Ferrari S, E Di Iorio, V Barbaro, D Ponzin, FS Sorrentino and F Parmeggiani. (2011). Retinitis pigmentosa: genes and disease mechanisms. Curr Genomics 12:238-49.

12. Griffith J, 3rd, K Sioufi, L Wilbanks, GN Magrath, EAT Say, MJ Lyons, M Wilkes, GS Pai and MMW Peterseim. (2022). Inherited Retinal Dystrophy in Southeastern United States: Characterization of South Carolina Patients and Comparative Literature Review. Genes (Basel) 13.

13. Nguyen XT, M Talib, C van Cauwenbergh, MJ van Schooneveld, M Fiocco, J Wijnholds, JB Ten Brink, RJ Florijn, NE Schalij-Delfos, G Dagnelie, MM van Genderen, E de Baere, MA Meester-Smoor, J De Zaeytijd, I Balikova, AA Thiadens, CB Hoyng, CC Klaver, LI van den Born, AA Bergen, BP Leroy and CJF Boon. (2021). CLINICAL CHARACTERISTICS AND NATURAL HISTORY OF RHO-ASSOCIATED RETINITIS PIGMENTOSA: A Long-Term Follow-Up Study. Retina 41:213-223.

14. Fahim A. (2018). Retinitis pigmentosa: recent advances and future directions in diagnosis and management. Curr Opin Pediatr 30:725-733.

15. Schwartz SD, JP Hubschman, G Heilwell, V Franco-Cardenas, CK Pan, RM Ostrick, E Mickunas, R Gay, I Klimanskaya and R Lanza. (2012). Embryonic stem cell trials for macular degeneration: a preliminary report. Lancet 379:713-20.

16. Ho AC, TS Chang, M Samuel, P Williamson, RF Willenbucher and T Malone. (2017). Experience With a Subretinal Cell-based Therapy in Patients With Geographic Atrophy Secondary to Age-related Macular Degeneration. Am J Ophthalmol 179: 67-80.

17. Occelli L, F Marinho, R Singh, F Binette, I Nasonkin and S Petersen-Jones. (2021). Subretinal Transplantation of Human Embryonic Stem Cell-Derived Retinal Tissue in a Feline Large Animal Model. JoVe (Journal of Visualized Experiments) 174.

18. Singh RK, LM Occelli, F Binette, SM Petersen-Jones and IO Nasonkin. (2019). Transplantation of Human Embryonic Stem Cell-Derived Retinal Tissue in the Subretinal Space of the Cat Eye. Stem Cells Dev 28:1151-1166.

19. Lin B, BT McLelland, RB Aramant, BB Thomas, G Nistor, HS Keirstead and MJ Seiler. (2020). Retina Organoid Transplants Develop Photoreceptors and Improve Visual Function in RCS Rats With RPE Dysfunction. Invest Ophthalmol Vis Sci 61:34.

20. Kashani AH, JS Lebkowski, FM Rahhal, RL Avery, H Salehi-Had, W Dang, C-M Lin, D Mitra, D Zhu, BB Thomas, ST Hikita, BO Pennington, LV Johnson, DO Clegg, DR Hinton and MS Humayun. (2018). A bioengineered retinal pigment epithelial monolayer for advanced, dry age-related macular degeneration. Sci.Transl. Med. 10:eaao4097.

21. Al-Nawaiseh S, F Thieltges, Z Liu, C Strack, R Brinken, N Braun, M Wolschendorf, A Maminishkis, N Eter and BV Stanzel. (2016). A Step by Step Protocol for Subretinal Surgery in Rabbits. J Vis Exp.

22. Sharma R, V Khristov, A Rising, BS Jha, R Dejene, N Hotaling, Y Li, J Stoddard, C Stankewicz, Q Wan, C Zhang, MM Campos, KJ Miyagishima, D McGaughey, R Villasmil, M Mattapallil, B Stanzel, H Qian, W Wong, L Chase, S Charles, T McGill, S Miller, A Maminishkis, J Amaral and K Bharti. (2019). Clinical-grade stem cell-derived retinal pigment epithelium patch rescues retinal degeneration in rodents and pigs. Sci Transl Med 11.

23. Zerti D, G Hilgen, B Dorgau, J Collin, M Ader, L Armstrong, E Sernagor and M Lako. (2021). Transplanted pluripotent stem cell-derived photoreceptor precursors elicit conventional and unusual light responses in mice with advanced retinal degeneration. Stem Cells 39:882-896.

24. Waldron PV, F Di Marco, K Kruczek, J Ribeiro, AB Graca, C Hippert, ND Aghaizu, AA Kalargyrou, AC Barber, G Grimaldi, Y Duran, SJI Blackford, M Kloc, D Goh, E Zabala Aldunate, RD Sampson, JWB Bainbridge, AJ Smith, A Gonzalez-Cordero, JC Sowden, RR Ali and RA Pearson. (2018). Transplanted Donor- or Stem Cell-Derived Cone Photoreceptors Can Both Integrate and Undergo Material Transfer in an Environment-Dependent Manner. Stem Cell Reports 10:406-421.

25. Radtke ND, RB Aramant, HM Petry, PT Green, DJ Pidwell and MJ Seiler. (2008). Vision improvement in retinal degeneration patients by implantation of retina together with retinal pigment epithelium. Am J Ophthalmol 146:172-182.

26. Seiler MJ and RB Aramant. (2012). Cell replacement and visual restoration by retinal sheet transplants. Prog Retin Eye Res 31:661-87.

27. Kuwahara A, C Ozone, T Nakano, K Saito, M Eiraku and Y Sasai. (2015). Generation of a ciliary margin-like stem cell niche from self-organizing human retinal tissue. Nat Commun 6:6286.

28. Eiraku M, N Takata, H Ishibashi, M Kawada, E Sakakura, S Okuda, K Sekiguchi, T Adachi and Y Sasai. (2011). Self-organizing optic-cup morphogenesis in three-dimensional culture. Nature 472:51-6.

29. Capowski EE, K Samimi, SJ Mayerl, MJ Phillips, I Pinilla, SE Howden, J Saha, AD Jansen, KL Edwards, LD Jager, K Barlow, R Valiauga, Z Erlichman, A Hagstrom, D Sinha, VM Sluch, X Chamling, DJ Zack, MC Skala and DM Gamm. (2019). Reproducibility and staging of 3D human retinal organoids across multiple pluripotent stem cell lines. Development 146:dev171686.

30. Wahlin KJ, JA Maruotti, SR Sripathi, J Ball, JM Angueyra, C Kim, R Grebe, W Li, BW Jones and DJ Zack. (2017). Photoreceptor Outer Segment-like Structures in Long-Term 3D Retinas from Human Pluripotent Stem Cells. Sci Rep 7:766.

Stem Cells and Development

Survival and functional integration of human embryonic stem cell-derived retinal organoids after shipping and transplantation into retinal degeneration rats (DOI: 10.1089/scd.2023.0257)

31. Singh RK, RK Mallela, PK Cornuet, AN Reifler, AP Chervenak, MD West, KY Wong and IO Nasonkin. (2015). Characterization of Three-Dimensional Retinal Tissue Derived from Human Embryonic Stem Cells in Adherent Monolayer Cultures. Stem Cells Dev 24:2778-95.

32. Zhong X, C Gutierrez, T Xue, C Hampton, MN Vergara, LH Cao, A Peters, TS Park, ET Zambidis, JS Meyer, DM Gamm, KW Yau and MV Canto-Soler. (2014). Generation of three-dimensional retinal tissue with functional photoreceptors from human iPSCs. Nat Commun 5:4047.

33. Singh RK, PA Winkler, F Binette, SM Petersen-Jones and IO Nasonkin. (2021). Comparison of Developmental Dynamics in Human Fetal Retina and Human Pluripotent Stem Cell-Derived Retinal Tissue. Stem Cells Dev 30:399-417.

34. Lin B, BT McLelland, A Mathur, RB Aramant and MJ Seiler. (2018). Sheets of human retinal progenitor transplants improve vision in rats with severe retinal degeneration. Exp Eye Res 174:13-28.

35. Singh RK, F Binette, M Seiler, SM Petersen-Jones and IO Nasonkin. (2021). Pluripotent Stem Cell-Based Organoid Technologies for Developing Next-Generation Vision Restoration Therapies of Blindness. J Ocul Pharmacol Ther 37:147-156.

36. Aramant RB and MJ Seiler. (2002). Retinal transplantation--advantages of intact fetal sheets. Prog Retin Eye Res 21:57-73.

37. Seiler MJ and RB Aramant. (1998). Intact sheets of fetal retina transplanted to restore damaged rat retinas. Invest Ophthalmol Vis Sci 39:2121-31.

38. Banin E, A Obolensky, M Idelson, I Hemo, E Reinhardtz, E Pikarsky, T Ben-Hur and B Reubinoff. (2006). Retinal incorporation and differentiation of neural precursors derived from human embryonic stem cells. Stem Cells 24:246-57.

39. Seiler MJ, RE Lin, BT McLelland, A Mathur, B Lin, J Sigman, AT De Guzman, LM Kitzes, RB Aramant and BB Thomas. (2017). Vision Recovery and Connectivity by Fetal Retinal Sheet Transplantation in an Immunodeficient Retinal Degenerate Rat Model. Invest Ophthalmol Vis Sci 58:614-630.

40. Foik AT, GA Lean, LR Scholl, BT McLelland, A Mathur, RB Aramant, MJ Seiler and DC Lyon. (2018). Detailed Visual Cortical Responses Generated by Retinal Sheet Transplants in Rats with Severe Retinal Degeneration. J Neurosci 38:10709-10724.

41. Seiler MJ, BB Thomas, Z Chen, R Wu, SR Sadda and RB Aramant. (2008). Retinal transplants restore visual responses: trans-synaptic tracing from visually responsive sites labels transplant neurons. Eur J Neurosci 28:208-20.

42. Seiler MJ, RB Aramant, BB Thomas, Q Peng, SR Sadda and HS Keirstead. (2010). Visual restoration and transplant connectivity in degenerate rats implanted with retinal progenitor sheets. Eur J Neurosci 31:508-20.

43. McLelland BT, B Lin, A Mathur, RB Aramant, BB Thomas, G Nistor, HS Keirstead and MJ Seiler. (2018). Transplanted hESC-Derived Retina Organoid Sheets Differentiate, Integrate, and Improve Visual Function in Retinal Degenerate Rats. Invest Ophthalmol Vis Sci 59:2586-2603.

44. Seiler MJ, RB Aramant, MK Jones, DL Ferguson, EC Bryda and HS Keirstead. (2014). A new immunodeficient pigmented retinal degenerate rat strain to study transplantation of human cells without immunosuppression. Graefes Arch Clin Exp Ophthalmol 252:1079-92.

45. Martinez-Navarrete G, MJ Seiler, RB Aramant, L Fernandez-Sanchez, I Pinilla and N Cuenca. (2011). Retinal degeneration in two lines of transgenic S334ter rats. Exp Eye Res 92:227-37.

46. LaVail MM, S Nishikawa, RH Steinberg, MI Naash, JL Duncan, N Trautmann, MT Matthes, D Yasumura, C Lau-Villacorta, J Chen, WM Peterson, H Yang and JG Flannery. (2018). Phenotypic characterization of P23H and S334ter rhodopsin transgenic rat models of inherited retinal degeneration. Exp Eye Res 167:56-90.

47. Singh RK, P Winkler, F Binette, RD Glickman, M Seiler, SM Petersen-Jones and IO Nasonkin. (2020). Development of a protocol for maintaining viability while shipping organoid-derived retinal tissue. J Tissue Eng Regen Med 14:388-394.

48. Kashani AH, J Uang, M Mert, F Rahhal, C Chan, RL Avery, P Dugel, S Chen, J Lebkowski, DO Clegg, DR Hinton and MS Humayun. (2020). Surgical Method for Implantation of a Biosynthetic Retinal Pigment Epithelium Monolayer for Geographic Atrophy: Experience from a Phase 1/2a Study. Ophthalmol. Retina 4:264-273.

49. Tu HY, T Watanabe, H Shirai, S Yamasaki, M Kinoshita, K Matsushita, T Hashiguchi, H Onoe, T Matsuyama, A Kuwahara, A Kishino, T Kimura, M Eiraku, K Suzuma, T Kitaoka, M Takahashi and M Mandai. (2019). Medium- to long-term survival and functional examination of human iPSC-derived retinas in rat and primate models of retinal degeneration. EBioMedicine 39:562-574.

50. Iraha S, HY Tu, S Yamasaki, T Kagawa, M Goto, R Takahashi, T Watanabe, S Sugita, S Yonemura, GA Sunagawa, T Matsuyama, M Fujii, A Kuwahara, A Kishino, N Koide, M Eiraku, H Tanihara, M Takahashi and M Mandai. (2018). Establishment of Immunodeficient Retinal Degeneration Model Mice and Functional Maturation of Human ESC-Derived Retinal Sheets after Transplantation. Stem Cell Reports 10:1059-1074.

51. Mandai M, M Fujii, T Hashiguchi, GA Sunagawa, S Ito, J Sun, J Kaneko, J Sho, C Yamada and M Takahashi. (2017). iPSC-Derived Retina Transplants Improve Vision in rd1 End-Stage Retinal-Degeneration Mice. Stem Cell Reports 8:69-83.

Figure Legends:

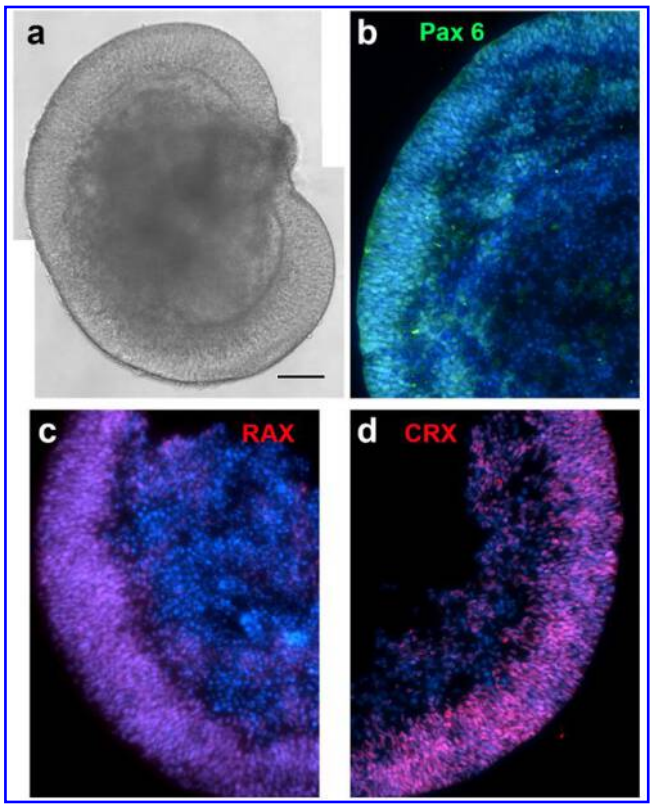

Figure 1. Selected images of young retinal organoids (day ~65-70) before surgeries (brightfield image, a, and immunohistochemical characterization of selected ROs at day 70). DAPI was used for nuclear counterstaining.

a) Phase contrast image of organoid differentiated for 70 days. Scale = 100 µm. **b)** outer organoid layer expresses transcription factors pax 6 (important for early eye development). **c)** Staining for early retinal transcription factor RAX (retinal homeobox protein Rx). **d)** staining for CRX (cone-rod-homeobox protein), a transcription factor for photoreceptor development.

Stem Cells and Development
Survival and functional integration of human embryonic stem cell-derived retinal organoids after shipping and transplantation into retinal degeneration rats (DOI: 10.1089/scd.2023.0257)

Stem Cells and Development

Survival and functional integration of human embryonic stem cell-derived retinal organoids after shipping and transplantation into retinal degeneration rats (DOI: 10.1089/scd.2023.0257)

This paper has been peer-reviewed and accepted for publication, but has yet to undergo copyediting and proof correction. The final published version may differ from this proof.

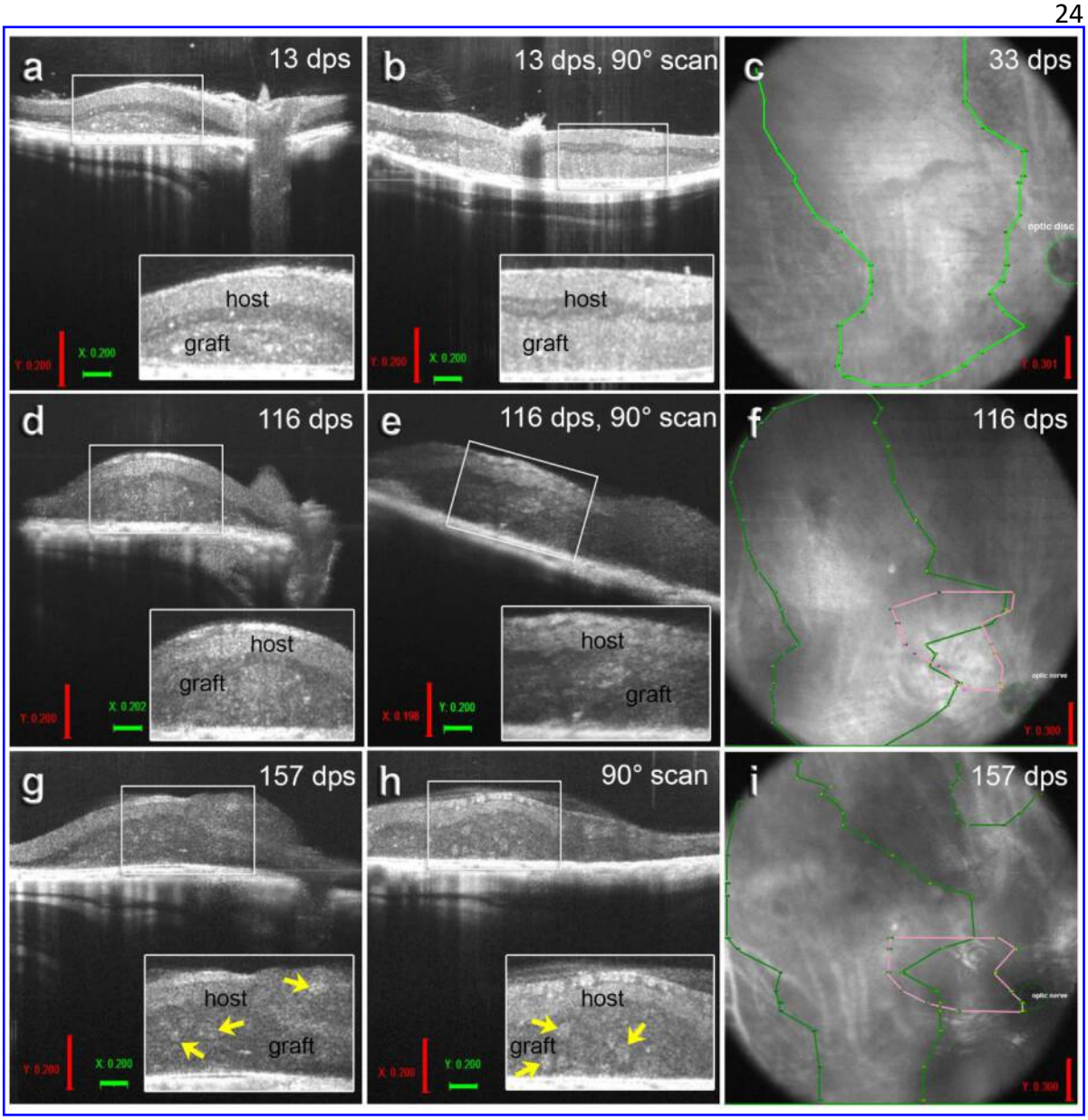

Figure 2. **Optical coherence tomography of transplant 1. a), b) 13 days post-surgery (dps).** **a)** B-scan showing transplant nasal to optic disc. **b)** B-scan turned 90° through the whole extent of subretinal transplant. Some blood on retinal surface. Boxes indicate area of enlargement in inserts. Scales = 200 µm. **c) Fundus image at 33 dps** with transplant outline (in green). The outline was deducted from corresponding B-scans. The optic disc is indicated by a green dashed circle. **d), e), f) 116 dps. d)** B-scan showing transplant at optic disc which has also grown onto the retinal surface. **e) B**-scan turned by 90°. Whitish area in center of enlargement indicates photoreceptor rosette. **f)** Fundus image at 116 dps with outline of subretinal transplant (in green). The extent of the epiretinal transplant is indicated in pink. **g) h), i) 157 dps. g)** B-scan showing transplant at optic disc which has also grown onto the

retinal surface. **h)** B-scan turned by 90°. The yellow arrows indicate photoreceptor rosettes. **i)** Fundus image at 157dps with outline of subretinal transplant (in green). The extent of the epiretinal transplant is indicated in pink.

Stem Cells and Development
Survival and functional integration of human embryonic stem cell-derived retinal organoids after shipping and transplantation into retinal degeneration rats (DOI: 10.1089/scd.2023.0257)
This paper has been peer-reviewed and accepted for publication, but has yet to undergo copyediting and proof correction. The final published version may differ from this proof.

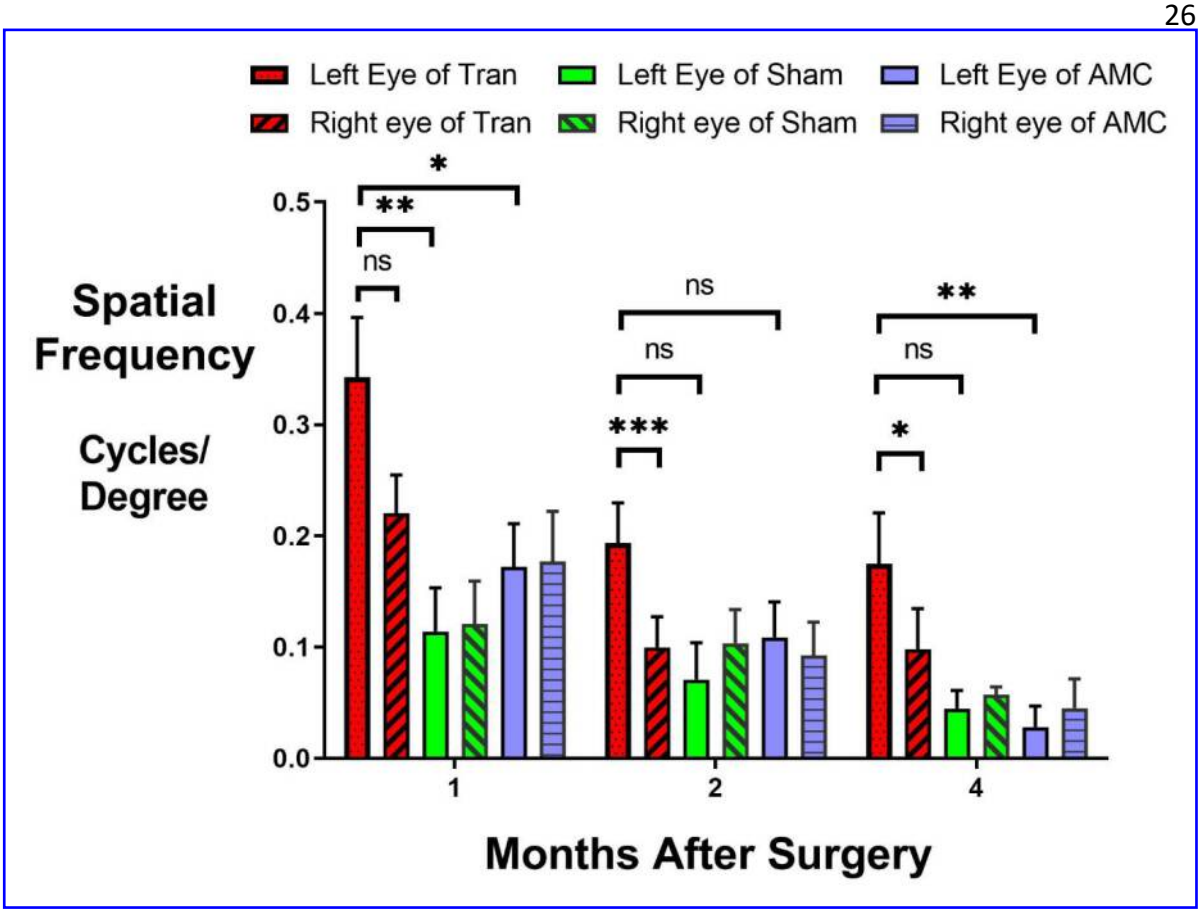

Figure 3: OKT - Visual acuity testing over time (up to 4 months post-surgery) shows significant better visual acuity in the eyes with transplants (red, dotted), but not in their non-surgery fellow eyes (red, striped), and sham-transplanted (green) or/and age-matched control (blue) eyes. * = p< 0.05; ** = p< 0.01. ns = non-significant.

Stem Cells and Development
Survival and functional integration of human embryonic stem cell-derived retinal organoids after shipping and transplantation into retinal degeneration rats (DOI: 10.1089/scd.2023.0257)
This paper has been peer-reviewed and accepted for publication, but has yet to undergo copyediting and proof correction. The final published version may differ from this proof.

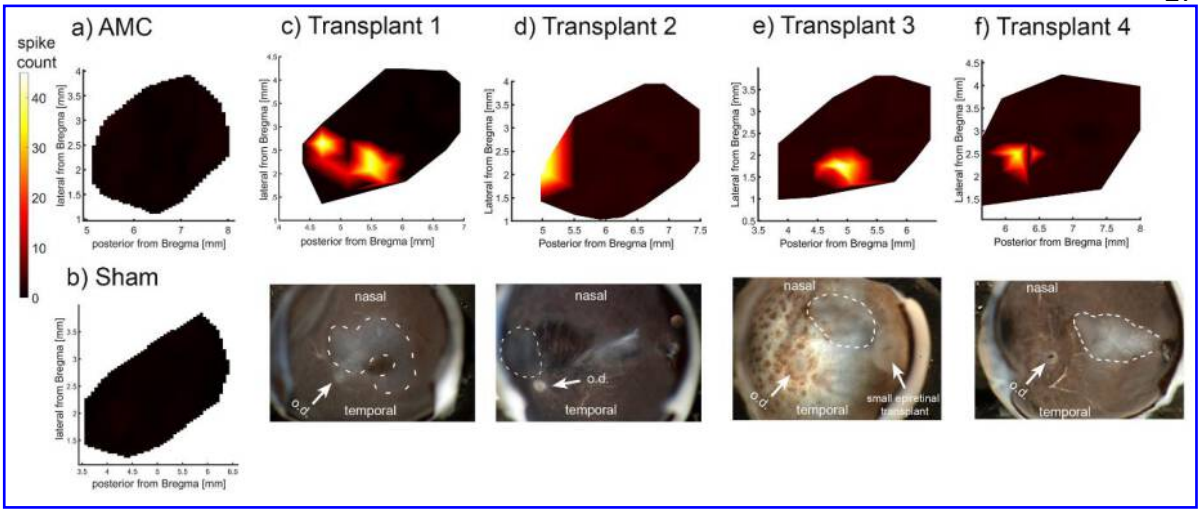

Figure 4. **Heat map of visual responses in superior colliculus** at 5.3-7.5 months after subretinal grafting (see Supplemental Table 2): **a)** Age-matched non-surgery control (AMC). **b)** sham surgery shows no responses. **c)-f)** Four rats with hESC-RO grafts: top row visual response heat maps; bottom row: images of dissected eye cups indicating the position of the transplants (dotted line). o.d. = optic disc

Stem Cells and Development
Survival and functional integration of human embryonic stem cell-derived retinal organoids after shipping and transplantation into retinal degeneration rats (DOI: 10.1089/scd.2023.0257)
This paper has been peer-reviewed and accepted for publication, but has yet to undergo copyediting and proof correction. The final published version may differ from this proof.

Stem Cells and Development
Survival and functional integration of human embryonic stem cell-derived retinal organoids after shipping and transplantation into retinal degeneration rats (DOI: 10.1089/scd.2023.0257)

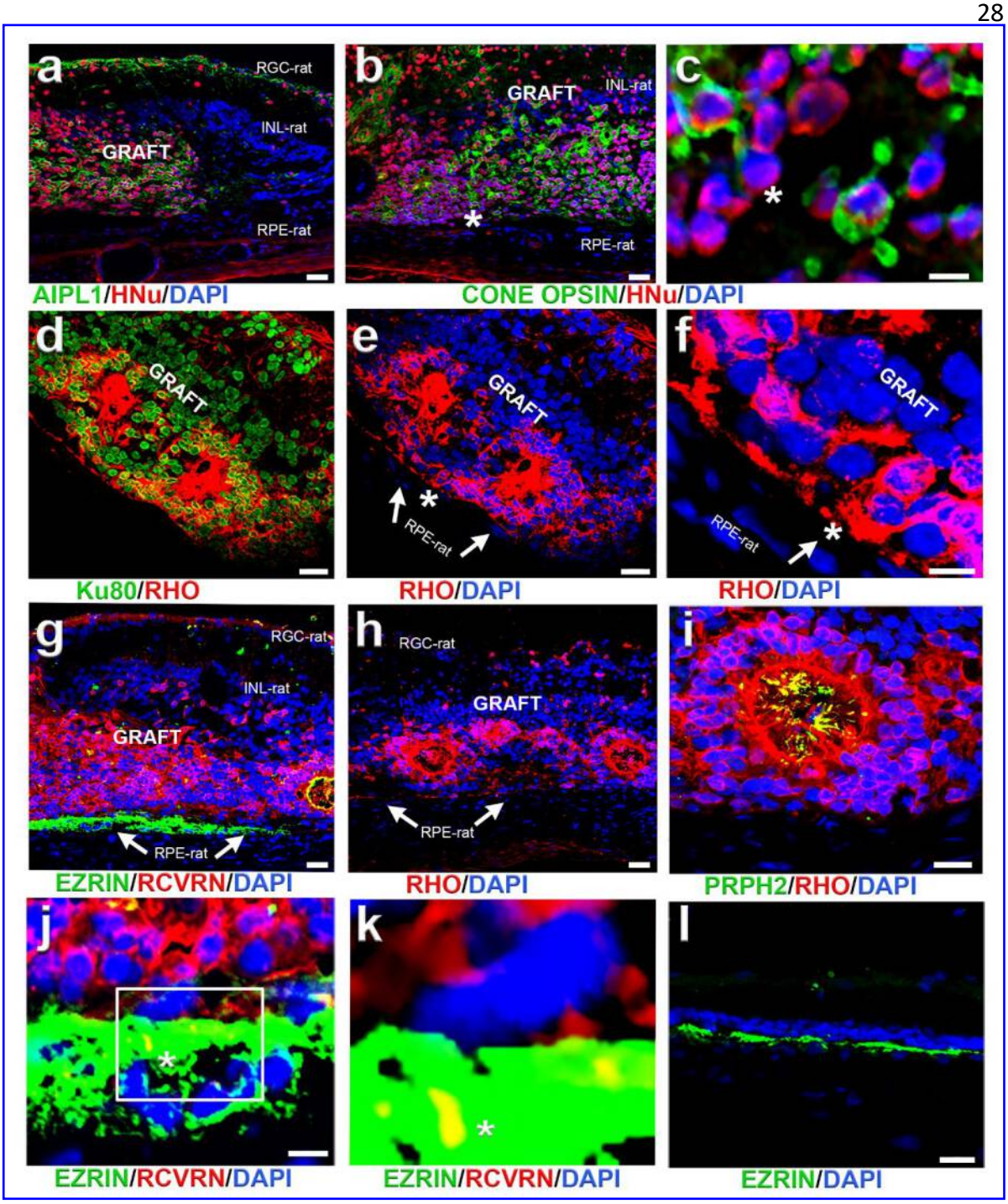

Figure 5. Photoreceptor development in grafts and interaction with RPE. **a-c**). Abundance of mature human photoreceptors in grafts. Immunohistochemistry with markers for human nuclei (HNu), in combination with photoreceptor marker AIPL1 (= aryl hydrocarbon receptor interacting protein like 1) or cone opsin. **d-e)** Abundance of human photoreceptors in grafts (marker rhodopsin). **g)-l)** interaction with host RPE (Ezrin). **i)** Graft photoreceptors express marker peripherin (PRPH2). Bars = 20 µm (a, b, d, e, I, l); = 10 µm (c, f, j).

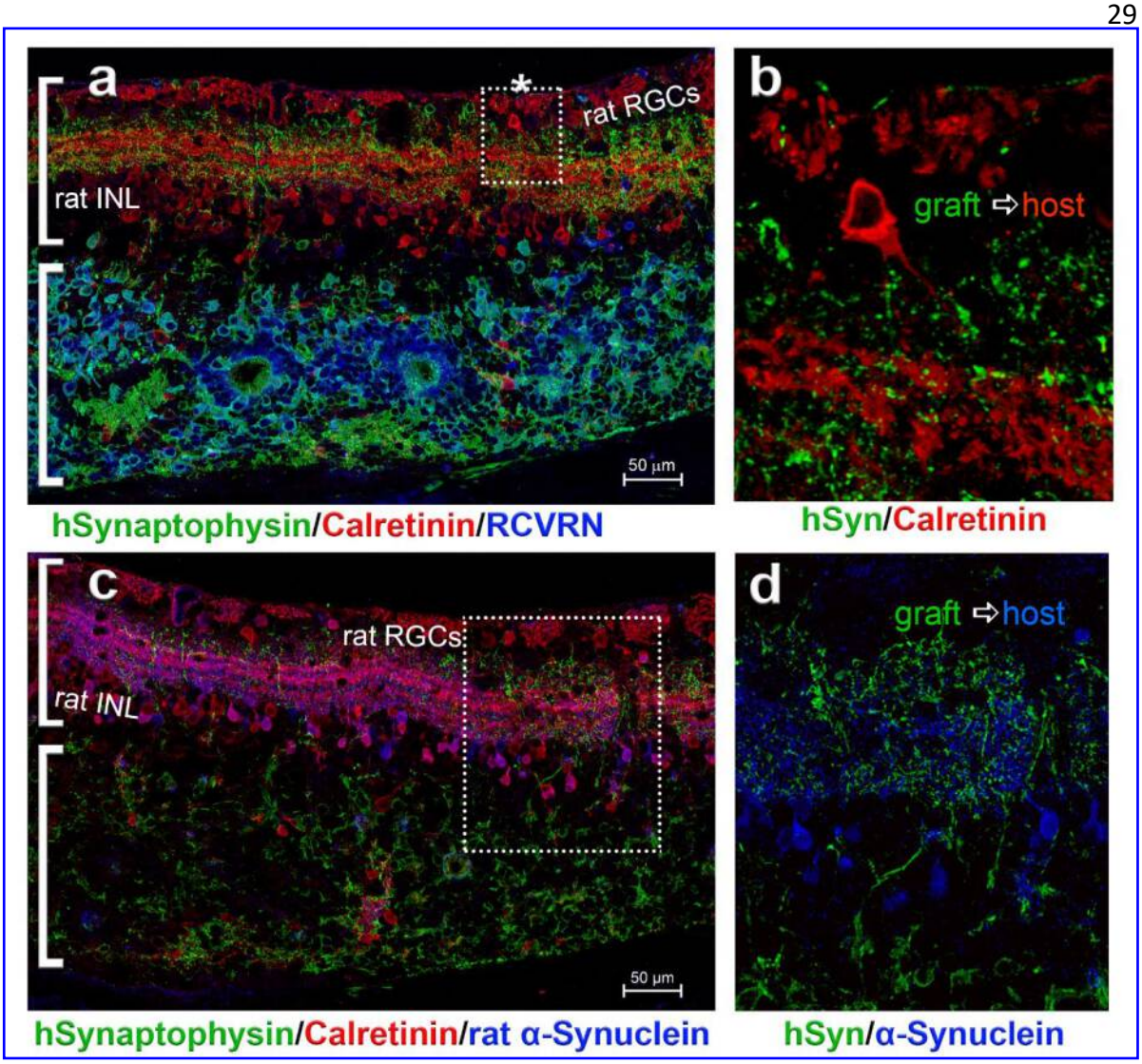

Figure 6: Synaptic connectivity graft – host (transplant 1, 160dps). **(a, b)** Combination of human-specific synaptophysin (hSyn) (green) with host markers Calretinin (red) and recoverin (RCVRN) (blue, **(a)**) or rat-specific α-synuclein (blue) **(c,d)** shows processes in the inner plexiform layer of the host. Bars = 50 µm.

Stem Cells and Development
Survival and functional integration of human embryonic stem cell-derived retinal organoids after shipping and transplantation into retinal degeneration rats (DOI: 10.1089/scd.2023.0257)
This paper has been peer-reviewed and accepted for publication, but has yet to undergo copyediting and proof correction. The final published version may differ from this proof.

Stem Cells and Development

Survival and functional integration of human embryonic stem cell-derived retinal organoids after shipping and transplantation into retinal degeneration rats (DOI: 10.1089/scd.2023.0257)

This paper has been peer-reviewed and accepted for publication, but has yet to undergo copyediting and proof correction. The final published version may differ from this proof.

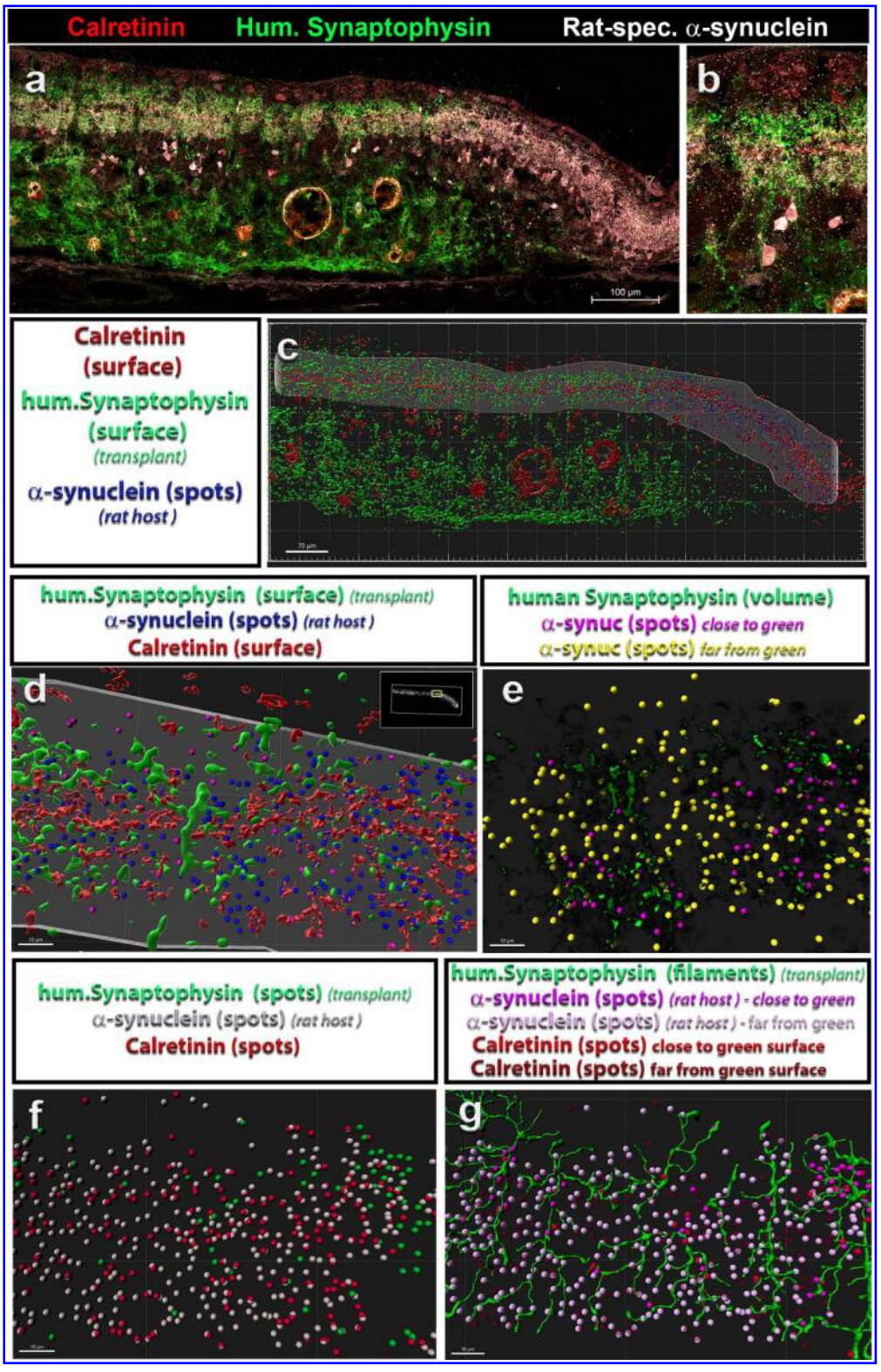

Figure 7. **Evaluating interaction of human synaptophysin processes in the host inner plexiform layer** (IPL) (Imaris software). Colocalization with Calretinin and rat-specific α-synuclein at 5.3 months after grafting (transplant 1). This rat had a response in the SC. **a)** overview image showing transplant with rosettes; Calretinin = red, human

synaptophysin = green, rat-specific α-synuclein = white. **b)** area of enlargement of rat host IPL. **c), d)** combination of human synaptophysin (surface) with α-synuclein (spots) and Calretinin (surface). **c)** selection of rat host IPL area for analysis. d) enlargement, tilted. **e)** human synaptophysin volume (green), with α-synuclein (spots) (close to green [1 µm or less] = magenta; far from green = yellow). **f)** combination of human synaptophysin spots (green) with α-synuclein spots (grey) and Calretinin spots (red). **g)** human synaptophysin filaments (green) in combination with α-synuclein spots (magenta) and Calretinin spots (red). Colors of spots are differentiated for their location close to or far away from the human synaptophysin green surface. f) g) are taken from same section as shown in Fig. 6b. Bars = 50 µm.

Stem Cells and Development
Survival and functional integration of human embryonic stem cell-derived retinal organoids after shipping and transplantation into retinal degeneration rats (DOI: 10.1089/scd.2023.0257)
This paper has been peer-reviewed and accepted for publication, but has yet to undergo copyediting and proof correction. The final published version may differ from this proof.

Stem Cells and Development

Survival and functional integration of human embryonic stem cell-derived retinal organoids after shipping and transplantation into retinal degeneration rats (DOI: 10.1089/scd.2023.0257)

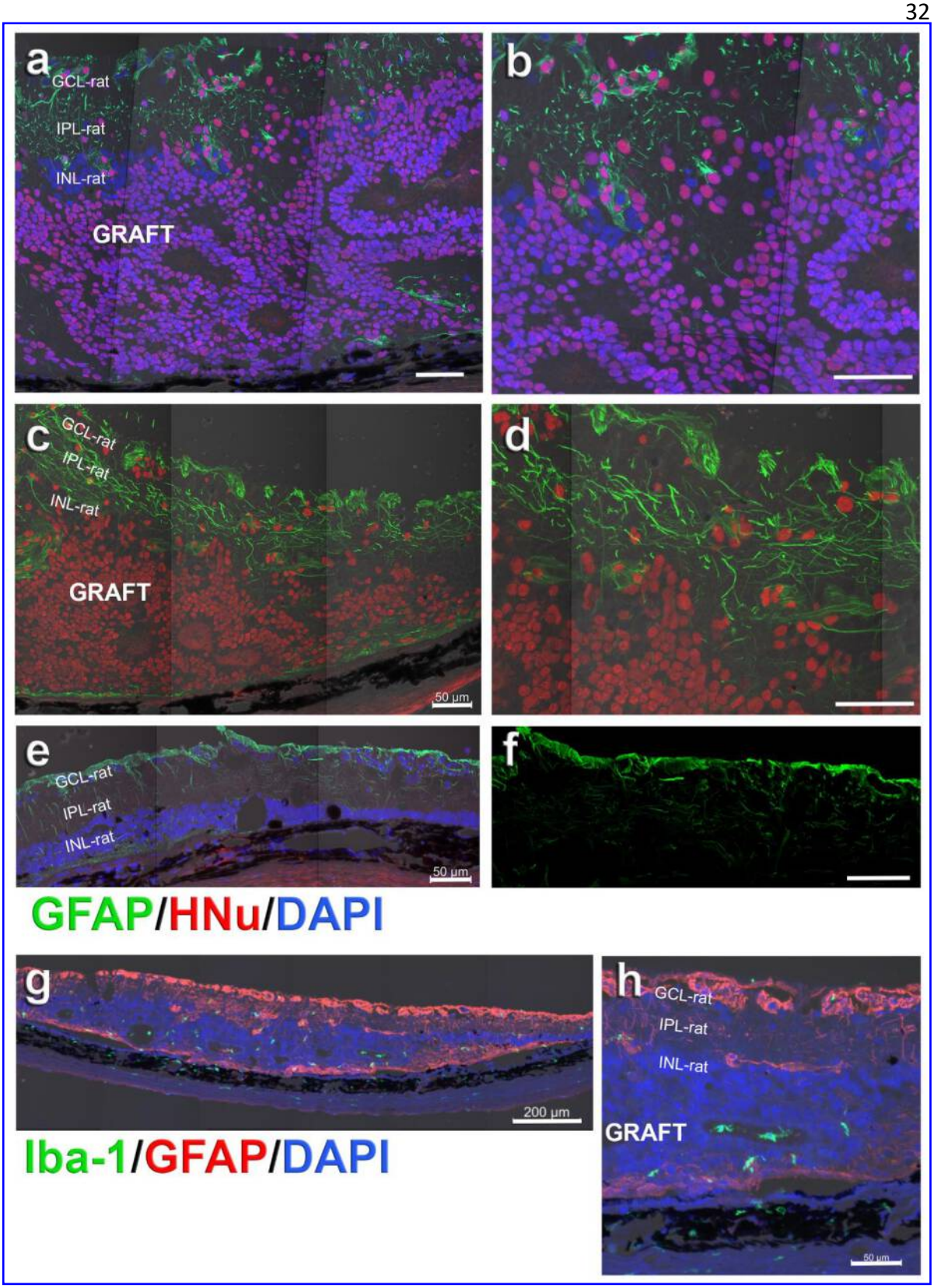

Figure 8: Analysis of host and graft glial and microglial cells (GFAP and Iba-1 staining). a, b) Transplant #9, 211 dps, age 239d. This rat was not recorded in the SC because of cornea

issues. Combination of GFAP (green) and human nuclei (red). b) shows enlargement of a). Dense network of glial processes. Note that there is almost no GFAP staining in the body of the transplant. c), d) Transplant #4, 211 dps, age 266d. This rat had a response in the SC. Combination of GFAP (red) and Iba-1 (microglia, red). Low concentration of microglial cells. Note that there are some microglial cells in the lumen of a photoreceptor rosette in h). Bars = 50 µm in a) – f), h); 200 µm in g). GCL = ganglion cell layer; IPL = inner plexiform layer; INL = inner nuclear layer

Stem Cells and Development
Survival and functional integration of human embryonic stem cell-derived retinal organoids after shipping and transplantation into retinal degeneration rats (DOI: 10.1089/scd.2023.0257)
This paper has been peer-reviewed and accepted for publication, but has yet to undergo copyediting and proof correction. The final published version may differ from this proof.